Delft University of Technology

Magnetic particle tracking

A semi-algebraic solution

Buist, K. A.; Nijssen, T. M.J.

Important note
To cite this publication, please use the final published version (if applicable).
Please check the document version above.

Magnetic particle tracking: A semi-algebraic solution

K.A. Buist [a], T.M.J. Nijssen [b]

[a] Multiphase Reactors Group, Department of Chemical Engineering & Chemistry, Eindhoven University of Technology, P.O. Box 513, 5600 MB Eindhoven, the Netherlands
[b] Bioprocess Engineering, Department of Biotechnology, Delft University of Technology, P.O. Box 5, 2600 AA Delft, the Netherlands

HIGHLIGHTS

- Fast Semi-Algebraic solution method for Magnetic Particle Tracking for granular flow.
- Imposed motion and orientation of tracer with noise levels.
- Decomposition of problem in separate algebraic solutions.
- Error and speed analysis compared to non-linear optimization method.
- Stability test to steep gradients in motion.

ARTICLE INFO

ABSTRACT

Magnetic Particle Tracking (MPT) is a relatively new non-invasive measurement technique which is often used to study dense granular flow. Its basic principle relies on tracking the movement of a single magnetic tracer by means of measuring the magnetic field strength at a suitable distance from the tracer. By assumption of a magnetic dipole and the use of minimization techniques, both location and orientation of the tracer can be determined. MPT is therefore uniquely suited for the study of non-spherical particles. The performance of the localization is largely dependent on the signal-to-noise ratio and very often relies on nonlinear optimization techniques, as the definition of the magnetic field generated by a dipole is highly nonlinear and has five degrees of freedom. In this paper, we present a semi-algebraic solution by decoupling the estimation of the position and orientation in separate algebraic solutions. The two estimates are mutually dependent, necessitating an iterative approach between the two. The main benefits of this new approach is in the speed and robustness of the algorithm, which are much higher than for the classical constrained nonlinear optimization techniques.

1. Introduction

Granular flows are often encountered in the chemical and processing technologies, such as in fluidization, grinding, compaction, and handling in hoppers and chutes. This is not an exhaustive list, but all of these applications share the trait that the mechanics of the granular motion are a subject of great interest to both industry and academia. However, due to their opaque nature, obtaining information on the individual grains can be very difficult. In general, the available experimental techniques for opaque, dense granular flows in 3D can be divided into tomographic techniques and particle tracking techniques, each with their inherent up and downsides (Chaouki et al., 1997). Available tomographic techniques are X-ray tomography, Magnetic Resonance Imaging (MRI), and Electrical Capacitance Tomography (ECT). For particle tracking techniques, there are Positron Emission Particle Tracking (PEPT) (Windows-Yule et al., 2020), Radioactive Particle Tracking (RPT) (Rasouli et al., 2015), and Magnetic Particle Tracking (MPT) (Buist et al., 2014).

MPT relies on the tracking of a single magnetic particle, often a neodymium permanent magnet. MPT originates from use in the medical field to study the motility tract (Richert et al., 2006). Due to lower costs relative to other tracking systems, MPT has gained more interest for the study of granular flows, in particular for the study of fluidization (Mema et al., 2020; Buist et al., 2014; Yang et al., 2017; Sette et al., 2015; Köhler et al., 2017; Patterson et al., 2010) and rotating equipment such as rotating drums, granulators, shear cells, and mills (Zhang et al., 2018; Neuwirth et al., 2013; Wu et al., 2021; Tao et al., 2019; Böttcher et al., 2021; Nijssen et al., 2022). The particles used in MPT are relatively heavy, which means the applicability of the technique has some limits related to the minimum size and density of the tracer.

MPT, however, comes with one additional benefit in that the magnetic field extending from the magnetic dipole is directional. Therefore, it is possible to simultaneously track position as well as orientation of the magnetic tracer (Buist et al., 2015). As such it is very suited for studying granular flows that are subject to large amounts of friction and rotation, as well as non-spherical particles (Buist et al., 2017). The sensors that are used in tracking the tracer can be divided in two types, being either Anisotropic Magneto Resistive (AMR) (Richert et al., 2006) or Hall effect sensors (Halow et al., 2012). Both types measure the magnetic field strength in the direction of the sensor, therefore tri-axis sensors are often used to determine the local magnetic field. A set of sensors is then positioned around a region of interest such that multiple indications of the magnetic field are obtained. The minimum number of sensors used is equal to the number of degrees of freedom, being 3 for position and 2 for orientation, since the magnetic dipole is symmetric along the line connecting the two poles. Finally, if the magnetic moment of the magnet is unknown as well this would require a sixth sensor.

Analysis of the data obtained from the set of sensors relies on minimization of the error of an estimate of the magnetic field relative to the measured field, assuming a likely position and orientation. Because this is a highly nonlinear problem, accuracy and speed of the optimization technique are a consideration to be made. But more importantly, because these techniques often rely on gradient descent methods, both local minima and solutions outside the physical domain are common problems. In a previous effort, constrained optimization techniques have been used to restrict the solution and force the solution to a physically feasible solution. Wu et al. (2021) have developed a semi-analytical solution to the problem and employed a deep neural network to filter the oversampled data set to achieve the best possible solution.

In this paper we present a new analysis technique that we term, in line with Wu et al. (2021): semi-algebraic. It relies on the fact that the magnetic field can be split into two parts, one relating to the distance between the sensor and the particle, and a second part relating to the orientation of the particle. The distance-related part can be treated as a multilateration problem, similar to the problems encountered in Global Positioning Systems (GPS). An algebraic solution is available for determination of the tracer position from a set of tracer-sensor distances, which will be discussed in the following section. The part associated with the orientation of the tracer is a linear problem as well. Both parts, however, rely on a reasonable estimate of the other, which means that an iterative procedure is needed to drive the solution to optimization. The final algorithm does incur a penalty in terms of accuracy, but is very stable and much faster than the nonlinear optimization techniques. Because of its inherent stability and speed, it can be used as an online monitoring tool during experimentation and as initialization for the more accurate nonlinear problem statement.

2. Method

Magnetic Particle Tracking relies on the reconstruction of the magnetic field stemming from a magnetic dipole. The magnetic field at any position is a function of the distance to and orientation of the dipole, and is given by the following equation:

$$\vec{H}(\vec{e}_p, \vec{r}_{ps}) = \frac{\mu_m}{4\pi}\left(-\frac{\vec{e}_p}{|\vec{r}_{ps}|^3} + \frac{3(\vec{e}_p \cdot \vec{r}_{ps})\vec{r}_{ps}}{|\vec{r}_{ps}|^5}\right) \tag{1}$$

2.1. Classic optimization

Traditionally, the solution to the problem of the magnetic field strength measured at each sensor is solved using nonlinear opti-

mization solvers. The use of a nonlinear solver is needed because solving for position and orientation is a nonlinear problem and it cannot be easily linearized.

In a first strategy, the Levenberg–Marquardt (LM) algorithm was used, which is an unconstrained technique for nonlinear problems. LM is also known as a dampened least-square method, iterating between the Gauss–Newton method and the method of gradient descent. The downside is that LM finds a local minimum and will have small gradients in the limit of small signals and high signal-to-noise ratios. This often leads to either a sub-optimal solution (local minimum) or large overshoots with solutions outside of the region of interest.

Therefore, in earlier work, constrained optimization techniques were used, such as Sequential Quadratic Programming (SQP). This allows for constraining of both the solution of the position within the predetermined domain, as well as the magnitude of the normal of the particle orientation to 1. For example, in case of a cylindrical domain:

$$\sqrt{x^2 + y^2} < R$$
$$h_1 \leqslant z \leqslant h_2 \tag{2}$$

$$|\vec{e}_p| = 1 \tag{3}$$

The second important component to the solution strategy is the choice of the objective function to be minimized by the optimization solvers. The first option is a relatively simple sum-of-squares error of the sensor signal:

$$Q = \sum_{i=1}^{N}(S_i - S_{t,i})^2 \tag{4}$$

in which, $S_t = H(\vec{e}_p, \vec{r}_{ps}) \cdot \vec{e}_s$. This quality function Q can be further refined by accounting for stray magnetic fields through addition of a gradiometer $\langle S \rangle$, and weighting with the standard deviation of the signal in the sensor σ_{S_i} for improved noise resilience.

$$Q = \sum_{i=1}^{N}\frac{\left[(S_i - \langle S \rangle) - (S_{t,i} - \langle S_t \rangle)\right]^2}{\sigma_{S_i}^2} \tag{5}$$

A second, more stable option for the quality function is the use of a probability function. This is a method that optimizes the probability of finding a particular value of the sensor S_t given the actual value S and its standard deviation σ_S.

$$P = \frac{1}{N}\sum_{i=1}^{N}\mathrm{erf}\left(\frac{S_i - S_{t,i}}{\sigma_{S_i}}\right) \tag{6}$$

The added benefit of the probability function is that it is bound between 0 and 1, whereas the quality function is only positive finite. Secondly, due to the fact that it minimizes the probability function it is less susceptible to multiple local minima in the domain (Buist et al., 2015). For the purpose of this paper we will use this final form of the quality function, Eq. 6.

2.2. Semi-algebraic

Eq. 1 can be further simplified by factoring out the distance from the position of the tracer towards the sensor $(|\vec{r}_{ps}|^3)$:

$$\vec{H}(\vec{e}_p, \vec{r}_{ps}) = \frac{\mu_m}{4\pi|\vec{r}_{ps}|^3}\left(-\vec{e}_p + 3(\vec{e}_p \cdot \vec{e}_{ps})\vec{e}_{ps}\right) \tag{7}$$

The resulting equation is dependent on the tracer-sensor distance cubed and a projection of the orientation of the tracer onto the directional vector of the tracer position to the sensor position $(\vec{e}_{ps})$, somewhat similar to as encountered in the work of Norrdine et al. (2016).

Note how the magnitude of $(-\vec{e}_p + 3(\vec{e}_p \cdot \vec{e}_{ps})\vec{e}_{ps})$ is bound between a value of 1 and 2. This means that with any estimate of the orientation of the tracer, the relative distance from the tracer to any sensor can be estimated within a factor $(1/2) \cdot (2^{1/3} - 1) \approx 13\%$.

This only holds in the ideal situation of no noise in the measured signal.

Looking at Eq. 7, we can now decompose the equation into a part only dependent on distances between the sensors and the tracer, and a part that is dependent on the orientation of the tracer and the positional direction vector ($\vec{e}_{ps}$) of the tracer to each sensor. The first part of the problem is a multilateration problem, very similar to GPS localization, and the second part is a linear function in the orientation of the tracer. Both parts have algebraic solutions, which we will discuss in the next two sections. The problems are, however, mutually dependent and thus iteration between the two algebraic sub-solutions is necessary.

2.2.1. Position

The determination of the position of the tracer follows the assumption that the relative distance between the tracer and each sensor is known. Of course, upon the first evaluation we must employ a rough estimate of the distance, but with iteration between this solution and the solution for orientation, increasingly accurate estimates are obtained. In this work we will make use of the approach as explained in Norrdine et al. (1315). Here we provide a brief explanation.

Given the positions of all sensors as $\vec{p}_{s,i}$ and the estimate of the distance $|\hat{r}_{ps,i}|$ between the sensor position and tracer position (x, y, z), the solution of the following problem must be found:

$$(x - p_{s_x,i})^2 + (y - p_{s_y,i})^2 + (z - p_{s_z,i})^2 = |r_{ps,i}|^2 \tag{8}$$

This can be rearranged to give:

$$x^2 + y^2 + z^2 - 2x \cdot p_{s_x,i} - 2y \cdot p_{s_y,i} - 2z \cdot p_{s_z,i}$$
$$= |r_{ps,i}|^2 - p_{s_x,i}^2 - p_{s_y,i}^2 - p_{s_z,i}^2 \tag{9}$$

Or in a matrix representation:

$$\begin{bmatrix} 1 & -2p_{s_x,i} & -2p_{s_y,i} & -2p_{s_z,i} \end{bmatrix} \begin{bmatrix} x^2 + y^2 + z^2 \\ x \\ y \\ z \end{bmatrix} = \begin{bmatrix} |\vec{r}_{ps,i}|^2 - |\vec{p}_{s,i}|^2 \end{bmatrix} \tag{10}$$

Which is the known general representation:

$$A \cdot \vec{p} = b \tag{11}$$

Where A is solely dependent on the information contained in the location of the sensors and b is the set of tracer-sensor distances minus the distances of the sensors to the origin. The solution of the position $\vec{p}$ for on the arbitrary number of sensors ($N \geqslant 3$) is a well known solution strategy following the Moore–Penrose inverse of A, providing a least squared solution to $\vec{p}$:

$$\hat{p} = A^+ b \tag{12}$$

with $A^+ = (A^T A)^{-1} A^T$. Additionally, one could use a weighted least-squares method where $A^+ = (A^T V^{-1} A)^{-1} A^T V^{-1}$ with V the covariance matrix of random errors. In this paper the use of weighing is not further explored, with one exception. Since the accuracy of the estimate of the distance to the sensor scales with r^{-3} and the solution $\hat{p}$ should be a least-squares fit with the measurement of the magnetic field strength, the solution must be weighted with $V^{-1} = |\vec{r}_{ps,i}|^6$.

2.2.2. Orientation

From the estimate of position using the above multilateration problem, the positional unit vector of the tracer towards each sensor i is defined:

$$\vec{e}_{ps,i} = \frac{\vec{p}_{s,i} - \vec{p}_p}{|\vec{r}_{ps,i}|} \tag{13}$$

We define the scaled magnetic field at the sensor position as:

$$\vec{e}'_h(\vec{e}_p, \vec{e}_{ps}) = -\vec{e}_p + 3(\vec{e}_p \cdot \vec{e}_{ps})\vec{e}_{ps} \tag{14}$$

which is calculated from the sensor values as:

$$\vec{e}'_{h,i} = \vec{H}_i \frac{4\pi|\vec{r}_{ps,i}|^3}{\mu} \tag{15}$$

Note that $\vec{e}'_h$ is not a unit vector, but does contain only orientational information and has a magnitude bound between 1 and 2. Eq. 14 can be written in matrix form as:

$$\begin{bmatrix} -1 + 3e_{ps,x}^2 & 3e_{ps,y} \cdot e_{ps,x} & 3e_{ps,z} \cdot e_{ps,x} \\ 3e_{ps,x} \cdot e_{ps,y} & -1 + 3e_{ps,y}^2 & 3e_{ps,z} \cdot e_{ps,y} \\ 3e_{ps,x} \cdot e_{ps,z} & 3e_{ps,y} \cdot e_{ps,z} & -1 + 3e_{ps,z}^2 \end{bmatrix} \begin{bmatrix} e_{p,x} \\ e_{p,y} \\ e_{p,z} \end{bmatrix} = \begin{bmatrix} e'_{h,x} \\ e'_{h,y} \\ e'_{h,z} \end{bmatrix} \tag{16}$$

Or in the known form as Eq. 11 above, where A can be defined as:

$$A = 3\vec{e}_{ps} \otimes \vec{e}_{ps} - I_3 \tag{17}$$

Eq. 16 can be defined at all sensors and will provide a single estimate for the orientation vector $\vec{e}_p$. Due to the nature of the least-squares method, this estimate is not strictly a unit vector and normalization is needed.

Finally, it must be noted that Eq. 14 also contains some information on the position, through the directional unit vector $\vec{e}_{ps}$ following Eq. 13. After a first estimate of both position and orientation, this information needs to be taken into account when estimating a new position. This can be achieved in different manners with the following options:

$$\begin{align} \hat{e}_{ps} \cdot \vec{e}_{ps} &= 1 \\ \hat{e}_p \cdot \vec{e}_{ps} &= \hat{\alpha} \\ -\hat{e}_p + 3(\hat{e}_p \cdot \vec{e}_{ps})\hat{e}_{ps} &= \hat{e}'_h \\ -\hat{e}_p + 3(\hat{e}_p \cdot \hat{e}_{ps})\vec{e}_{ps} &= \hat{e}'_h \end{align} \tag{18}$$

Here, the hat notation denotes an estimate of that parameter. The vector $\vec{e}_{ps}$ is defined by Eq. 13, such that the position of the tracer is the free parameter. All above solutions provide an improvement of the estimate of the position, but the most simple one provides the best solution: $\hat{e}_{ps} \cdot \vec{e}_{ps} = 1$.

2.2.3. Iteration

Now that both sub-problems have been defined and each has a separate algebraic solution, the solution to the overall problem can be discussed. The solution to the problem of position, which relies on multilateration, is dependent on an estimate of $|\vec{e}'_{h,i}|$, which is dependent on the estimate of the orientation of the tracer. The distance of each sensor i to the tracer is then defined as:

$$|\vec{r}_{ps,i}| = \left(|\vec{H}_i| \frac{4\pi}{\mu|\vec{e}'_{h,i}|} \right)^{\frac{1}{3}} \tag{19}$$

in which $|\vec{e}'_{h,i}|$ is defined by Eq. 15.

The solution of the orientation depends on the positional unit vector $\vec{e}_{ps,i}$ as defined by Eq. 13, which depends on an estimate of the position. The mean value of $\langle 1, 2 \rangle = 1.5$ can be used as a first estimate of $|\vec{e}'_{h,i}|$, which is within 13 % accuracy. For consecutive iterations, a previous estimate of the orientation can be used. Subsequent iterations between position and orientation will lead to

the best estimate of the two. We have found that in most cases 2 to 3 iterations suffice. For simplicity we have chosen to only set a fixed number of iterations to 10, to ensure an optimal solution is found. As for many optimization algorithms, it is entirely possible to implement stopping criteria based on the quality of the solution, even further increasing the numerical efficiency.

3. Numerical Setup

To test the new semi-algebraic method, a relatively simple numerical setup is used. 24 tri-axis sensors are paired in groups of 4 rings, with inner diameter of 0.32 m and distance of 0.12 m between each ring, each ring containing 6 sensors. The vertical component of the tri-axis sensor is always pointing down. The sec-

Table 1
Parameter and settings describing the numerical setup.

Number of sensor rings	4
Number of tri-axis sensors per ring	6
Ring diameter	0.32 m
Distance between rings	0.12 m
Magnetic moment tracer	0.014 A·m²
Amplitude Fermat spiral	0.02 m
Period Fermat spiral	5 π
Period x, y component orientation	32 π
Period z component orientation	64 π
Signal-to-noise ratio (SNR)	2–20
Moving average filter size	10
Step size for analysis	10

ond axis points either way or towards the origin, the third axis is orthogonal to the other two.

A predefined motion is imposed to a fictitious tracer particle and the true magnetic field at each sensor location is calculated. The predefined motion follows from a Fermat spiral using both branches with a linear change along the vertical axis. The orientation of the tracer follows from imposing a sinusoidal pattern to the respective components, sine for x, cosine for y and z (with different frequencies), and then normalizing the vector to unity magnitude. A total of $N_t = 10,000$ time steps are generated. Analysis is performed at every tenth step. All settings for the setup can be found in Table 1.

This choice of imposed motion is made to allow the tracer to traverse the entire region of interest. In principle, any other motion could be imposed, as long as it is relatively smooth. Because the nonlinear optimization technique is dependent on an initial guess of the position and orientation, large gradients and sudden changes in direction can be problematic, as will be shown later. Some techniques instead use Kalman filters to account for the heading of the tracer, which serves to stabilize the initialization problem. An overview of the position and orientation of both the sensors and fictitious tracer is provided in Fig. 1.

Noise is added to the generated magnetic field such that the signal-to-noise ratio (SNR) ranges from 2 to 20 with increments of 2. A simple moving average filter of size 10 is used to allow for some smoothing of the data, similar to filtering performed in a real MPT system. Subsequently, sampling is performed every 20 time steps.

The initialization of the nonlinear optimization is performed by providing the exact solution of the first time step. Note that in any
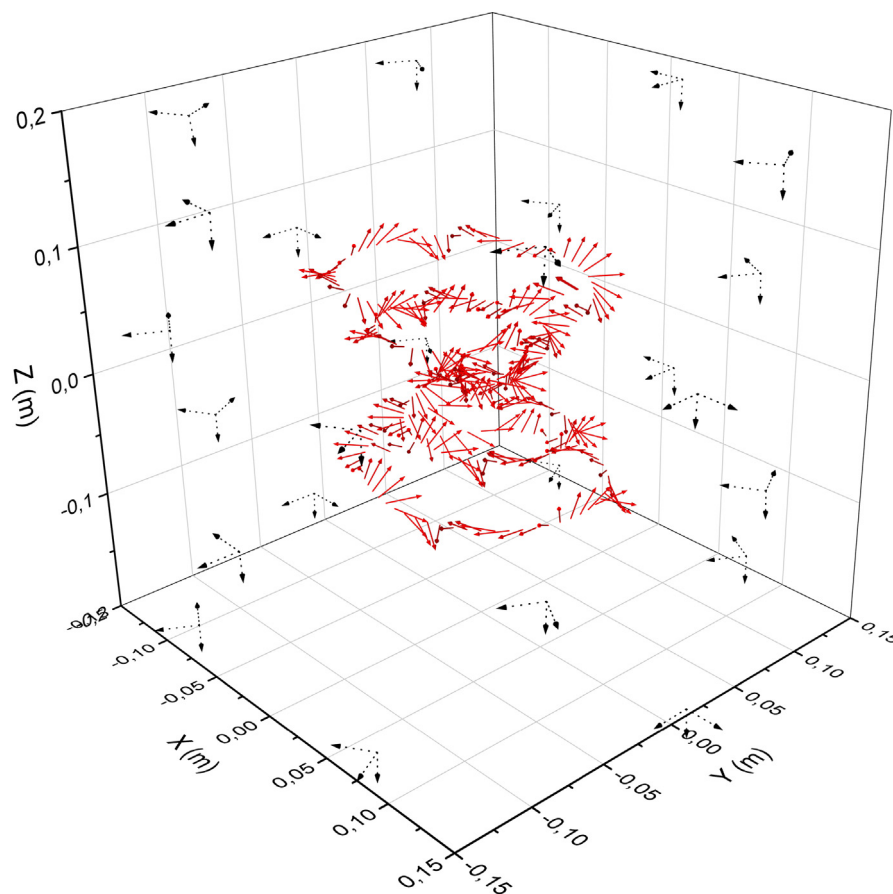

Fig. 1. Setup of the sensor array in black arrows and true position and orientation of the fictitious tracer in red arrows (only N_p=300 points shown).
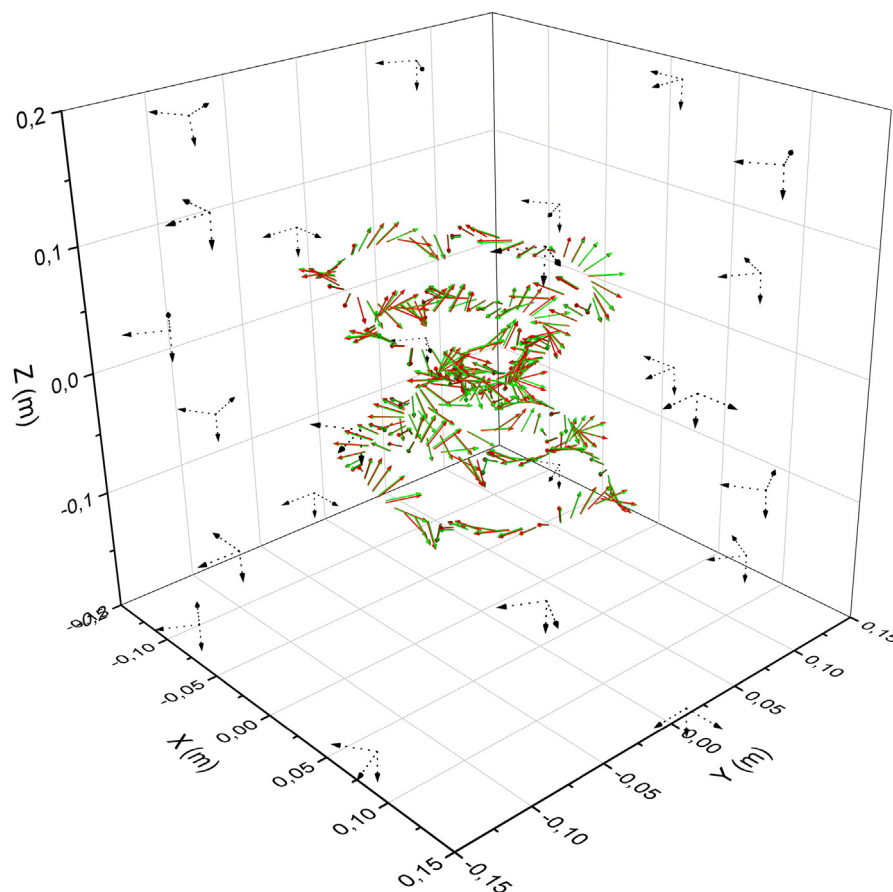
Fig. 2. Setup of the sensor array in black arrows, true position and orientation in red arrows, reconstructed position and orientation using semi algebraic solution at SNR = 20 in green arrows.

real experiment this estimate is unknown and often multiple guesses are tried to converge to a global minimum for the initialization. However, in this work the focus will be on the run time of the algorithm rather than the initialization, which is time consuming, but depending on the duration of an actual experiment, often not limiting. The semi-algebraic method is initialized by assuming a set of distances following Eq. 19 by assuming the scaled magnetic field $|\vec{e}'_{h,i}|$ to be of size 1.5.

4. Results

The purpose of the optimization techniques is to find the most probable position and orientation of the tracer and as such provide a reconstruction of the trajectory of the tracer. In Fig. 2 a reconstruction of the tracer position and orientation is provided for the case with SNR = 20 and the semi-algebraic solution. The semi-algebraic solution is clearly capable of providing a close resemblance to the trajectory at large signal to noise ratios.

To quantify the accuracy of the semi-algebraic solution and compare it to the nonlinear optimization technique using the probability function, the averaged error in position; the distance to the real position, and averaged error in orientation is determined for the entire set at each SNR.

Fig. 3a displays the error in position for the two techniques, which ranges from 1 cm to 1 mm for SNR = 2 to SNR = 20, respectively. Generally, the nonlinear optimization outperforms the semi-algebraic solution by 30 to 50 %, performing relatively better at lower signal-to-noise ratios. The dependence of the averaged

position error on the amount of noise is, however, nonlinear. The scaling of both the techniques is quite similar.

Fig. 3b displays the error in orientation for the two techniques, which ranges from 0.06 rad to 0.01 rad for SNR = 2 to SNR = 20. Also for the orientation the nonlinear optimization outperforms the semi-algebraic solution by 3 to 20%, performing relatively better at lower signal-to-noise ratios. Also here the dependency of the average angular error on the signal to noise ratio is nonlinear. The scaling of the noise for the semi-algebraic technique seems to be larger than the nonlinear optimization.

The main benefit, however, of the semi-algebraic technique is the average speedup, which averaged over all SNRs is a factor 31.7 ± 3.4. Secondly, because of the robust nature of the semi-algebraic technique, it does not have a tendency to show results outside or on the boundary of the physical domain. This significant speedup of the analysis allows for a quick, robust, and relatively accurate online measurement of position and orientation.

To further showcase the robustness of the semi-algebraic technique we have chosen to skip data points by increasing the step size of the analysis. The step size is changed from 10 to 200 time steps at a constant signal-to-noise ratio of 6. Figs. 4a and 4b show the averaged error in the position and orientation, respectively, as a function of the chosen step size. From these figures it can be seen that the error exhibited by the semi-algabraic algorithm remains mostly constant with increasing step size. The nonlinear optimization, however, shows a sudden increase in error around a step size of 100, after which the error becomes in the order of the maximum error. Since the nonlinear optimization method depends heavily on an estimate of the position and orientation obtained from the previous time step, it is very susceptible to large changes over time.
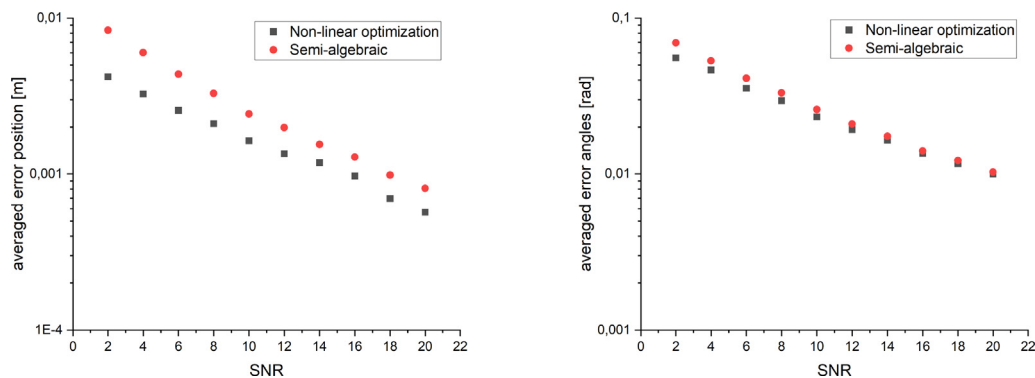
Fig. 3. (a) Averaged positional error in m as a function of the signal-to-noise ratio for the nonlinear solver and the semi-algebraic solver. (b) Averaged positional error in m as a function of the signal-to-noise ratio for the nonlinear solver and the semi-algebraic solver.
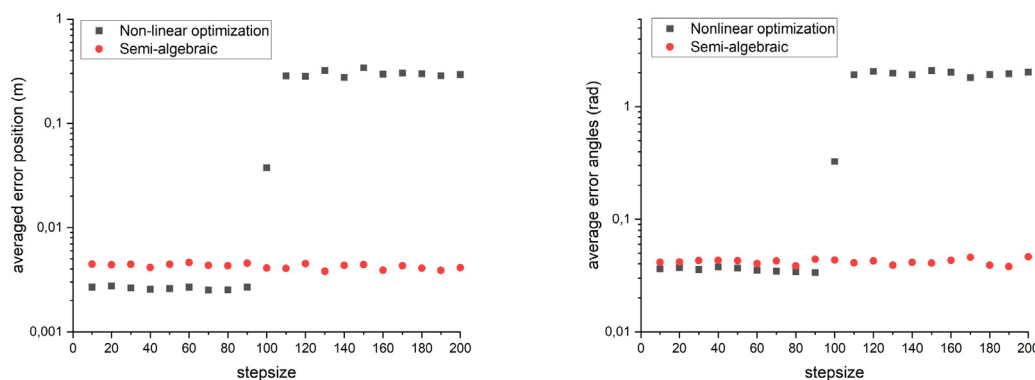

Fig. 4. (a) Averaged position error in meters as a function of the step size for the nonlinear solver and the semi-algebraic solver. (b) Averaged angular error in radians as a function of the step size for the nonlinear solver and the semi-algebraic solver.

Thus, when the current position and orientation changes too much with respect to the previous time step, the nonlinear optimization method is unable to find the global minimum and is therefore forced towards the boundaries/constraints of the problem. Typically it cannot recover from such a situation and in practice this forces the optimization method to perform a global search again, which is not done for this analysis. Performing one or multiple global optimizations is very time consuming. The semi-algebraic method can be completely independent from an estimate of a previous step and shows a near constant solution to the problem statement. It can therefore be used as an initial guess to the nonlinear optimization method, rather than finding a global solution. The main benefit is that no global searches, which are time consuming, are necessary even for the non-linear solver and that a reasonable estimate for the non-linear solver can always be provided. The consequence of having a reasonable and independent estimate for the non-linear solver is that the non-linear solver can be readily parallelized across multiple CPUs, which will allow speedup for the nonlinear solver as well. Secondly, because there is no need for sequentially solving the problem a vectorized approach of the semi-algebraic method could be possible.

5. Conclusions

In this paper, a new analysis technique for determination of the tracer position and orientation in a Magnetic Particle Tracking system is presented. This technique relies on the decomposition of the magnetic field in distance-dependent and an orientation-dependent parts. This decomposition allows for linearization of the two parts of the problem, enabling an algebraic least-squares solution of the two sub-problems. The distance-dependent part relates to multilateration, whereas the orientation-dependent part

is unique to the Magnetic Particle Tracking technique. The division of the problem into two algebraic solutions, however, requires an iterative approach between the two solutions.

This new semi-algebraic solution is evaluated over a wide range of signal-to-noise ratios and compared to the classical constrained nonlinear optimization technique. Results show that the semi-algebraic technique is significantly faster than the nonlinear optimization technique, but at the cost of loss of some accuracy. The new semi algebraic solution however does allow for fast and reasonably accurate real-time determination of the position and orientation of the tracer in MPT. The semi algebraic technique is also very robust, which can otherwise only partly be achieved by constraining the nonlinear optimization. Because of the speed of the semi algebraic solution, this technique is an ideal candidate for real-time monitoring and can serve as a first guess for nonlinear optimization. Furthermore, because the solution of the semi-algebraic method performs similarly to the non-linear method in terms of error propagation, the semi algebraic technique could be used as a fast optimization technique for the design of sensor arrays.

Declaration of Competing Interest

The authors declare that they have no known competing financial interests or personal relationships that could have appeared to influence the work reported in this paper.

References

Böttcher, A.C., Schilde, C., Kwade, A., 2021. Experimental assessment of grinding bead velocity distributions and stressing conditions in stirred media mills. Adv. Powder Technol. 32 (2), 413–423.

Buist, K.A., van der Gaag, A.C., Deen, N.G., Kuipers, J.A., 2014. Improved magnetic particle tracking technique in dense gas fluidized beds. AIChE J. 60 (9), 3133–3142.

Buist, K., Van Erdewijk, T., Deen, N., Kuipers, J., 2015. Determination and comparison of rotational velocity in a pseudo 2-d fluidized bed using magnetic particle tracking and discrete particle modeling. AIChE J. 61 (10), 3198–3207.

Buist, K.A., Jayaprakash, P., Kuipers, J., Deen, N.G., Padding, J.T., 2017. Magnetic particle tracking for nonspherical particles in a cylindrical fluidized bed. AIChE J. 63 (12), 5335–5342.

Chaouki, J., Larachi, F., Dudukovic, M., 1997. Non-invasive monitoring of multiphase flows. Elsevier.

Halow, J., Holsopple, K., Crawshaw, B., Daw, S., Finney, C., 2012. Observed mixing behavior of single particles in a bubbling fluidized bed of higher-density particles. Industr. Eng. Chem. Res. 51 (44), 14566–14576.

Köhler, A., Pallarès, D., Johnsson, F., 2017. Magnetic tracking of a fuel particle in a fluid-dynamically down-scaled fluidised bed. Fuel Process. Technol. 162, 147–156.

Mema, I., Buist, K.A., Kuipers, J., Padding, J.T., 2020. Fluidization of spherical versus elongated particles: Experimental investigation using magnetic particle tracking. AIChE J. 66 (4), e16895.

Neuwirth, J., Antonyuk, S., Heinrich, S., Jacob, M., 2013. Cfd–dem study and direct measurement of the granular flow in a rotor granulator. Chem. Eng. Sci. 86, 151–163.

Nijssen, T.M.J., Dijk, M.A.H., Kuipers, J.A.M., van der Stel, J., Adema, A.T., Buist, K.A., 2022. Experiments on floating bed rotating drums using magnetic particle tracking. AIChE J. 68 (5), 1–11. https://doi.org/10.1002/aic.17627.

Norrdine, A.: An algebraic solution to the multilateration problem. In: Proceedings of the 15th international conference on indoor positioning and indoor navigation, Sydney, Australia, vol. 1315 (2012).

Norrdine, A., Kasmi, Z., Blankenbach, J., 2016. A novel method for overcoming the impact of spatially varying ambient magnetic fields on a dc magnetic field-based tracking system. J. Locat. Based Serv. 10 (1), 3–15.

Patterson, E.E., Halow, J., Daw, S., 2010. Innovative method using magnetic particle tracking to measure solids circulation in a spouted fluidized bed. Industr. Eng. Chem. Res. 49 (11), 5037–5043.

Rasouli, M., Bertrand, F., Chaouki, J., 2015. A multiple radioactive particle tracking technique to investigate particulate flows. AIChE J. 61 (2), 384–394.

Richert, H., Kosch, O., Görnert, P., 2006. Magnetic Monitoring as a Diagnostic Method for Investigating Motility in the Human Digestive System. John Wiley & Sons, Ltd, pp. 481–498. chap. 4.2.

Sette, E., Pallarès, D., Johnsson, F., Ahrentorp, F., Ericsson, A., Johansson, C., 2015. Magnetic tracer-particle tracking in a fluid dynamically down-scaled bubbling fluidized bed. Fuel Process. Technol. 138, 368–377.

Tao, X., Tu, X., Wu, H., 2019. A new development in magnetic particle tracking technology and its application in a sheared dense granular flow. Rev. Sci. Instrum. 90 (6), 065116.

Windows-Yule, C., Seville, J., Ingram, A., Parker, D., 2020. Positron emission particle tracking of granular flows. Annu. Rev. Chem. Biomol. Eng. 11, 367–396.

Wu, H., Du, P., Kokate, R., Wang, J.X., 2021. A semi-analytical solution and ai-based reconstruction algorithms for magnetic particle tracking. Plos one 16 (7), e0254051.

Yang, L., Padding, J., Buist, K., Kuipers, J., 2017. Three-dimensional fluidized beds with rough spheres: Validation of a two fluid model by magnetic particle tracking and discrete particle simulations. Chem. Eng. Sci. 174, 238–258.

Zhang, L., Weigler, F., Idakiev, V., Jiang, Z., Mörl, L., Mellmann, J., Tsotsas, E., 2018. Experimental study of the particle motion in flighted rotating drums by means of magnetic particle tracking. Powder Technol. 339, 817–826.